1st International Seminar on Dam Protection against Overtopping and Accidental Leakage
M.Á. Toledo, R. Morán, E. Oñate (Eds)
Madrid, 24-25 November 2014

LABORATORY MEASUREMENTS AND NUMERICAL SIMULATIONS OF OVERTOPPING NAPPE IMPINGEMENT JETS

JOSÉ M. CARRILLO[1] AND LUIS G. CASTILLO[1]

[1]Universidad Politécnica de Cartagena (UPCT)
Paseo Alfonso XIII, 52
30203 Cartagena, Spain
e-mail: jose.carrillo@upct.es luis.castillo@upct.es

Key words: Impingement Jets, Laboratory, Numerical Simulations, Overtopping.

Summary. Rectangular jets constitute one of the energy dissipation methods in the overtopping of dams. The high turbulence and aeration phenomena that appear in falling jets and dissipation basins make it difficult to carry out studies based only on classical methodologies. There are studies modeling spillways with computational fluid dynamics (CFD) which produces accurate results. However, the study of overflow nappe impingement jets has not been sufficiently examined. Simulations of free air-water overflow weirs are scarce, and require small mesh sizes and a high computational effort. This work seeks to address such simulation. Results obtained with ANSYS CFX are compared with laboratory measurements and empirical formulae. Good agreement is obtained with experimental and theoretical data. Knowing the parameters analyzed, designers will be able to estimate the scour effects and the stability of the dam with a higher certainty.

1 INTRODUCTION

In recent years, the increasing magnitude of design floods has prompted re-evaluations of spillway capacity and operational scenarios for large dams throughout the world. Current capacity of many spillways is inadequate, raising the possibility that dams might be overtopped during extreme events. This creates new loading scenarios for the dam and raises questions about erosion and scour downstream from the dam (Wahl *et al.* [47]).

Nappe flow constitutes one of the types of plunge pool operation in the overtopping of dams. In turbulent flow, pressure fluctuations are the main mechanism affecting the incipient movement of the particles. The erodibility index relates the relative magnitude of the erosive capacity of water and relative resistance of the material (natural or artificial) to resist erosion (Annandale [3]). In order to obtain the right pool depth, the designer needs to know the magnitude, frequency and extent of the dynamic pressures on the pool floor as a function of the jet characteristics.

Different empirical formulae may be used to characterize the pressures in plunge pools. Due to the great difficulty of instrumenting prototypes, all of the formulae have been obtained by using diverse experimental facilities and reduced scale models. Research in plunge pools has been published by many authors including Moore [38], Albertson *et al.* [1], Horeni [29], Lencastre [31], Cola [20], Hartung and Häusler [27], Ervine and Falvey [21], Franzetti and

Tanda [24], Castillo ([9], [10], [11]), Withers [50], Puertas [40], Ervine *et al.* [22], Puertas and Dolz [41], Castillo *et al.* ([12], [13], [18], [19]), Bollaert [5], Bollaert and Schleiss ([6], [7]), Manso *et al.* ([33], [34]), Melo *et al.* [37], Federspiel [23], Castillo and Carrillo ([14], [15], [16], [17]), and Carrillo [8]. Recent studies in this field have been focused on scour formation. These include the studies carried out by Annandale ([2], [3]), Hoffmans [28], Asadollahi *et al.* [4] and Mehraein *et al.* [36]. Modeling of falling jets is difficult because the break-up and air entrainment characteristics of the jet are influenced by both surface tension and turbulence effects. In addition to this, the pressure fluctuation spectrum is also affected by the turbulence scale. In a physical model scale effects will appear. However, their effects may be minimized or accounted for through careful choice of the model size and careful interpretation of the results.

In falling jets and dissipation basins it is difficult to carry out studies based only on classical methodologies. The computational fluid dynamics (CFD) programs allow researchers and designers to evaluate different effects with a smaller cost than that incurred building scale models. There are studies modeling spillways with which produces accurate results. However, the study of overflow nappe impingement jets has not been sufficiently examined. Simulations of free air-water overflow weirs are scarce, and require small mesh sizes and a high computational effort.

In this paper, previous studies have been revised and complemented with new laboratory data obtained in a new installation of nappe flow. Pressure data at the bottom of the plunge pool have been obtained and compared using three different experimental facilities (i.e., data from Castillo [9] and Puertas [40], and data obtained in a new experimental facility).

Turbulence in the falling jet has been analyzed using computational fluid dynamics (CFD) techniques. Results obtained with ANSYS CFX are compared with laboratory measurements and empirical formulae. To identify the level of reliability of computed parameters, validation of air entrainment and velocity along free falling jets, thickness and break-up of jets, and pressures on the bottom of the plunge pool, are carried out by using a two-fluid model, turbulence models and mesh-size analysis.

2 EXPERIMENTAL FACILITY

2.1 Turbulent jet experimental facility

The hydraulics laboratory at the Universidad Politécnica de Cartagena in Spain has a turbulent jet experimental facility in which the energy dissipation of turbulent rectangular jets is being studied (Figure 1). The mobile mechanism allows researchers to vary the discharge heights between 1.70 and 4.00 m and flows from 10 to 150 l/s. It has an inlet channel with a length of 4 m and width of 0.95 m, in which different dissipation systems have been located. The weir is a sharp crest with a width of 0.85 m and height of 0.37 m.

The plunge pool, in which different water cushions may be regulated, is a 1.60 m high and 1.05 m wide box made of methacrylate. Instantaneous pressure measurements were registered with piezoresistive transducers located on the plunge pool bottom, kinetic energy at the inlet channel with Acoustic Doppler Velocimeter (ADV) equipment, mean velocities and air entrainment rate in different sections of the falling jet with optical fibre instrumentation.

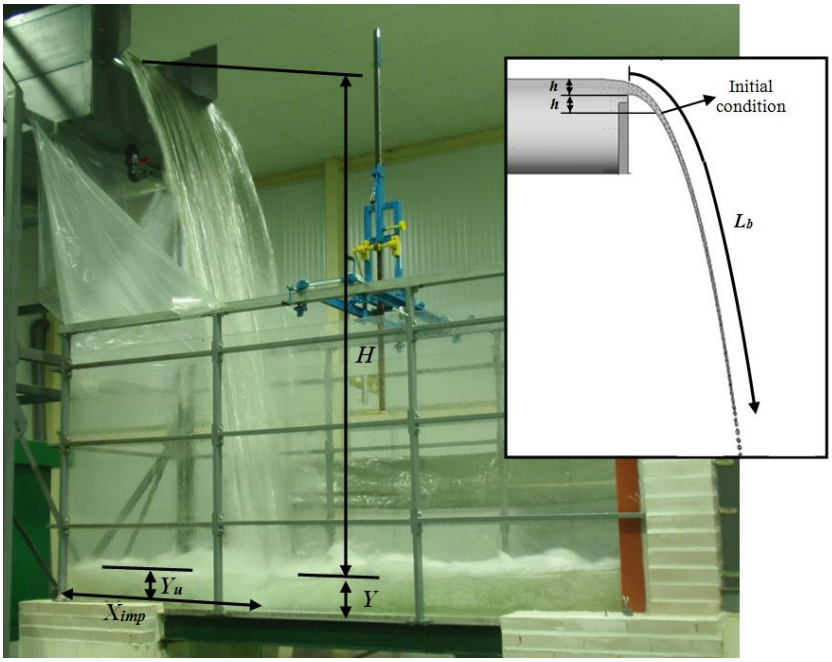

Figure 1: Device of turbulent jets

The flow was measured with a V-notch weir, located downstream from the plunge pool. The discharge rate of the V-notch was tested with a velocity-area method using ADV equipment upstream from the weir. Differences between V-notch results and the velocity-area method were smaller than 5% of the current flow.

Experiments carried out in this study correspond to different falling heights H between 1.70 m and 3.00 m, seven water cushion heights Y (from direct impact to 0.60 m) and seven specific flows q (from 0.020 to 0.064 m^2/s). Laboratory data cover a range of $0.60 \leq H/L_b \leq 2.02$, with L_b being the break-up length. Almost 190 registers were obtained, with each one being of 7200 points and with an acquisition rate of 20 samples per second.

2.2 Pressure transducers

With the aim of obtaining the instantaneous pressures, GE Druck model UNIK 5000 pressure transducers were used. The sensors were located on the bottom of the plunge pool, at the symmetry plane of the turbulent jet device and equally spaced at 5 cm intervals. These sensors have a pressure range between -200 and +800 mbar and a precision of ±0.04% of the full scale output. After carrying out a static calibration, the pressure precision of the transducers was ±0.01 water column meters. Instantaneous pressures were obtained by considering a frequency rate of 20 Hz and measurements of 360 s. In each measurement, seven sensors were used at the same time (one at the stagnation point, three upstream from the stagnation point, and three downstream). Each measurement was repeated three times.

2.3 Optical fibre equipment

To measure the mean velocity and the air entrainment at the falling jet, an RBI-instrumentation dual-tip probe optical phase-detection instrument was used. This equipment

enables measurement in water up to 20 m/s flow velocity and the relative uncertainty concerning the void fraction is estimated at about 15% (Stutz and Reboud [45], [46]). The rise and fall of the probe signal corresponds, respectively, to the arrival and the departure of the gas phase at the tip of the sensor.

The void fraction was defined as the ratio of the total time the probe is in gas (Σt_{Gi}) to the experiment duration time t. The mean velocity of the fluid was estimated by using a cross correlation technique between the signals obtained for the two tips. The accuracy of the velocity measurements performed under steady flow conditions was estimated at about ±10% for the velocity range analyzed (Stutz and Reboud [45], [46]).

2.4 The Acoustic Doppler Velocimeter (ADV)

ADVs have become highly useful in fluid dynamics and are applied to the study of three-dimensional flow and turbulence in both the laboratory and field (rivers, channels and hydraulic structures, amongst others).

The setting characteristics were selected considering that the main objective is to measure the mean velocity and macroscopic turbulence. In this way, the velocity range was selected as ±0.30 m/s with a frequency of 10 Hz, avoiding the noise generated by the equipment when higher frequencies are used. With this setting, the ADV equipment was able to measure the time-averaged flow field with an accuracy of better than ±0.002 m/s. The kinetic turbulence measured 0.50 m upstream the weir in the experimental facility was used as the inlet condition in the numerical simulations.

3 NUMERICAL MODELING

3.1 Considerations

For the turbulent flow, CFD codes solve the differential Reynolds-Averaged Navier-Stokes (RANS) equations of the phenomenon in the fluid domain, retaining the reference quantity in the three directions for each control volume identified. The equations for conservation of mass and momentum may be written as:

$$\frac{\partial \rho}{\partial t} + \frac{\partial}{\partial x_j}\left(\rho U_j\right) = 0 \tag{1}$$

$$\frac{\partial \rho U_i}{\partial t} + \frac{\partial}{\partial x_j}\left(\rho U_i U_j\right) = -\frac{\partial p}{\partial x_i} + \frac{\partial}{\partial x_j}\left(2\mu S_{ij} - \rho\overline{u_i' u_j'}\right) \tag{2}$$

where i and j are indices, x_i represents the coordinate directions (i = 1 to 3 for x, y, z directions, respectively), ρ the flow density, t the time, U the velocity vector, p the pressure, u_i' presents the turbulent velocity in each direction (i = 1 to 3 for x, y, z directions, respectively), μ is the molecular viscosity, S_{ij} is the mean strain-rate tensor and $-\rho\overline{u_i' u_j'}$ is the Reynolds stress.

Eddy-viscosity turbulence models consider that such turbulence consists of small eddies which are continuously forming and dissipating, and in which the Reynolds stresses are assumed to be proportional to mean velocity gradients. The Reynolds stresses may be related to the mean velocity gradients and eddy viscosity by the gradient diffusion hypothesis:

$$-\rho\overline{u_i' u_j'} = \mu_t \left(\frac{\partial U_i}{\partial x_j} + \frac{\partial U_j}{\partial x_i}\right) - \frac{2}{3}\delta_{ij}\left(\rho k + \mu_t \frac{\partial U_k}{\partial x_k}\right) \quad (3)$$

with μ_t being the eddy viscosity or turbulent viscosity, $k = 1/2\overline{u_i' u_i'}$ the turbulent kinetic energy and δ the Kronecker delta function.

In preparing this study, an extensive literature review of hydraulic dams was carried out. However, given that the CFD methodology is relatively recent there are few well documented references for free overflow spillways. For this reason, it is necessary to review CFD accuracy in similar typologies.

3.2 Numerical simulations

For the numerical modeling, the CFD volume finite scheme program ANSYS CFX has been used.

The fluid domain is divided into control volumes, which must satisfy the balance of the governing equations. The code allows different types of elements to be solved. The main difference between the types of elements is the number of nodes used to solve the equations within each control volume. A larger number of nodes per element obtains a more accurate solution in their internal resolution. Following Castillo *et al.* [19] and Carrillo [8], the mesh size was 0.01 m based on hexahedral elements, approximately the half of the impingement jet thickness for the tests carried out.

All scenarios were obtained by a transient calculation time of 60 seconds, using 20 Hz frequency, the same as used in the laboratory pressure measurements. The transient statistics were obtained by considering that permanent conditions are reached after 20 seconds of simulation.

In order to reach the closure of the Navier-Stoke equations, turbulence models can be used. There are different approximations, from one-equation turbulence models to the direct simulation.

As a compromise between accuracy and computational effort, the RANS turbulence models are widely used. Eddy-viscosity turbulence models consider that such turbulence consists of small eddies which are continuously forming and dissipating, and in which the Reynolds stresses are assumed to be proportional to mean velocity gradients.

Castillo *et al.* [19] and Carrillo [8] tested different turbulence models in the falling jet case. In this work, the SST turbulence model has been selected. The SST model takes into account the accuracy of the *k-ω* model in the near-wall region and the free stream independence of the *k-ε* model in the outer part of the boundary layer. To do this, the original *k-ω* model (Wilcox [49]) is multiplied by a blending function F_1, while the *k-ε* model (Launder & Sharma [30]) is transformed to a *k-ω* formulation and multiplied by a function 1- F_1 (Menter [35]). F_1 is designed to be one inside the boundary layer and decreases to a value of zero away from the surface.

In judging the convergence of a solution in a finite-volume scheme, a widely used method entails monitoring the residuals (Wasewar and Vijay Sarathi [48]). Residuals are defined as the imbalance in each conservation equation following each iteration. The solution is said to have converged if the scaled residuals are smaller than prefixed values ranging between 10^{-3} and 10^{-6}. In this work, the residual values were set to 10^{-4} for all the variables.

To solve the air-water two-phase flow, the Eulerian-Eulerian multiphase flow

homogeneous model was selected. In each control volume, the sum of the volume fraction of all phases is the unit.

In general, it may be assumed that the free surface is on the 0.5 air volume fraction. However, due to the high air entrainment in the nappe, the jet thickness and the break-up length were calculated using a 0.8 air volume fraction.

The model boundary conditions corresponded to the flow, the turbulence at the inlet condition obtained with ADV (located 0.50 m upstream of the weir), the upstream and downstream levels and their hydrostatic pressures distributions (Figure 2).

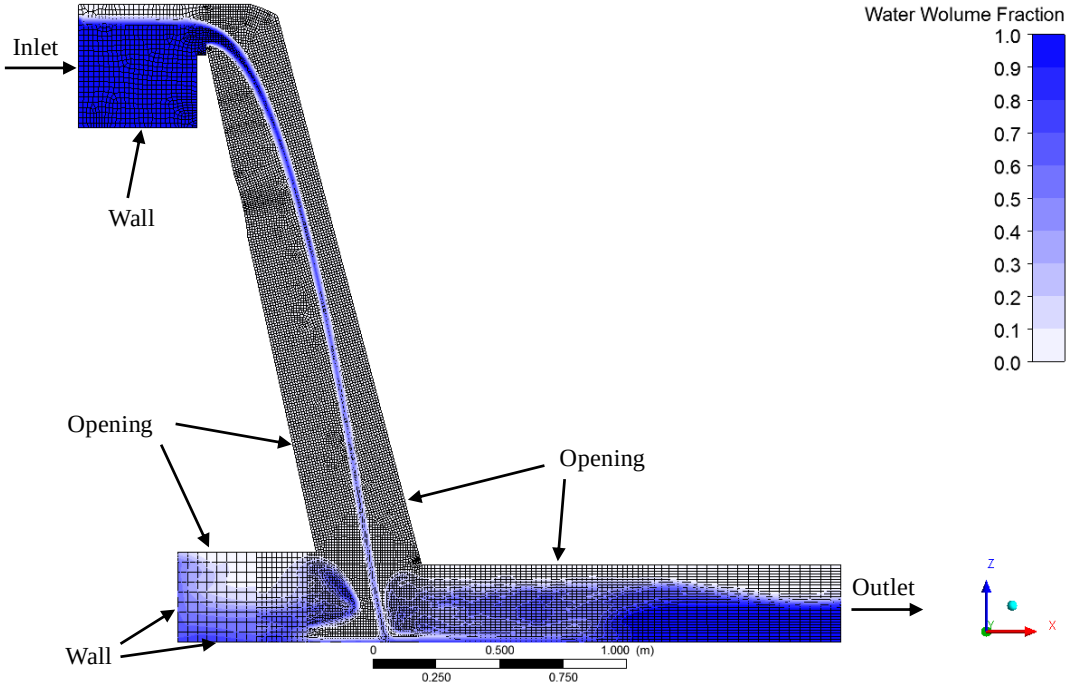

Figure 2: Scheme of boundary conditions

The inlet condition considers the mass flow rate with a normal direction to the boundary condition (q = 0.058 m^2/s, q = 0.037 m^2/s, q = 0.023 m^2/s), the turbulent kinetic energy (0.00036 m^2/s^2 for q = 0.058 m^2/s, 0.00019 m^2/s^2 for q = 0.037 m^2/s, 0.00011 m^2/s^2 for q = 0.023 m^2/s), and the water level height at upstream deposit (2.445 m for q = 0.058 m^2/s, 2.423 m for q = 0.037 m^2/s, 2.397 m for q = 0.023 m^2/s). For simplicity, the symmetry condition in the longitudinal plane of the plunge pool was used.

The outlet condition has been considered as an opening condition with flow normal to the boundary condition and hydrostatic pressure. The water level height at outlet has been modified according to the water cushion depth, Y, in the laboratory device.

For the walls of the upper deposit, the weir and the dissipation bowl, no slip wall conditions and smooth walls have been considered.

The atmosphere condition has been simulated as an opening condition with a relative pressure of 0 Pa, air volume fraction of 1 and water volume fraction of 0.

4 EMPIRICAL FORMULAE

Using instantaneous pressure registers obtained at the bottom of plunge pools, Castillo ([10], [11]) proposed estimators for the nappe flow case: the turbulence intensity at issuance conditions T_u, the jet break-up length L_b, the lateral spread distance ξ, the impingement thickness B_j, and the mean dynamic pressure coefficient C_p.

The turbulence intensity at issuance conditions for laboratory specific flow ($q < 0.25$ m^2/s) may be estimated as:

$$T_u^* = q^{0.43}/IC \tag{4}$$

with IC being the initial conditions with dimensions [$L^{0.86}\,T^{-0.43}$]:

$$IC = 14.95g^{0.50}/(K^{1.22}C_d^{0.19}) \tag{5}$$

where g is the gravity acceleration, K is a non-dimensional fit coefficient (≈ 0.85) and C_d is the discharge coefficient [$L^{0.5}\,T^{-1}$].

However, for prototype specific flows ($q >> 0.25$ m^2/s) a mean turbulence index is $T_u \sim 1.2$ % (Castillo [10]).

The designers need to know the height between the upstream water level and the downstream water level H, the impingement jet thickness B_j, the water cushion depth Y, and the jet break-up length L_b. In this way, the head mean may be calculated at the stagnation point of the plunge pool bottom H_m.

Following the results obtained by Ervine *et al.* [22] in circular jets, the jet break-up length in the rectangular jet case is calculated as (Castillo [10]):

$$\frac{L_b}{B_i F_i^2} = \frac{K}{\left(K_\varphi T_u F_i^2\right)^{0.82}} \tag{6}$$

with B_i, F_i and $T_u = \overline{V_i}'/V_i$ being the jet thickness, the Froude number and the turbulent intensity at issuance conditions, while K is a non-dimensional fit coefficient (≈ 0.85). $K_\varphi = \overline{V_i}'/w'$ is the turbulent parameter coefficient, where $\overline{V_i}'$ and w' are the root mean square (RMS) and the streamwise turbulent velocity component.

The impingement jet thickness is obtained with the following:

$$B_j = B_g + 2\xi = \frac{q}{\sqrt{2gH}} + 4\varphi\sqrt{h}\left[\sqrt{2H} - 2\sqrt{h}\right] \tag{7}$$

where H is the height between the upstream water level and the downstream water and $\varphi = K_\varphi\, T_u$ is the turbulence parameter in the nappe flow case.

The trajectory of the central nappe may be obtained with the Scimeni [44] formulation:

$$x^* = 2.155(z^* + 1)^{\frac{1}{2.33}} - 1 \tag{8}$$

where $x^* = x/h$ and $z^* = z/h$, with x and z being the coordinate axes considering the origin in the weir crest.

5 RESULTS AND DISCUSION

5.1 Mean dynamic pressure coefficient

The mean dynamic pressure coefficient C_p may be obtained as a function of Y/B_j and H/L_b rates. In this way, the instantaneous pressures signals obtained on the bottom of the plunge pools may be adjusted in curves for different ranges. Two cases were considered for the mean dynamic pressure coefficient.

For the non-effective water cushion ($Y \leq 5.5B_j$):

when $H/L_b \leq 1.00$:

$$C_p = 1 - 0.0014e^{5.755(H/L_b)} \quad (9)$$

when $H/L_b > 1.00$:

$$C_p = 14.643e^{-3.244(H/L_b)} \quad (10)$$

The energy dissipation is due to the air entraining into the falling jet and the depth of water standing upstream from the jet, while downstream from the stagnation point the cushion does not influence the energy dissipation. Exponential adjustments have been obtained, with regression coefficients R^2 of 0.97 and 0.91 for $H/L_b < 1.00$ and $H/L_b \geq 1.00$, respectively.

For the effective water cushion ($Y > 5.5B_j$), in Figure 3 data are compared with the formula obtained by Cola [20] for non-aerated rectangular jets. As the Cola formula considers the mean pressure instead of the mean dynamic pressure, the curve has been modified to consider the relation $C_p = f(Y/B_j)$ without the water cushion.

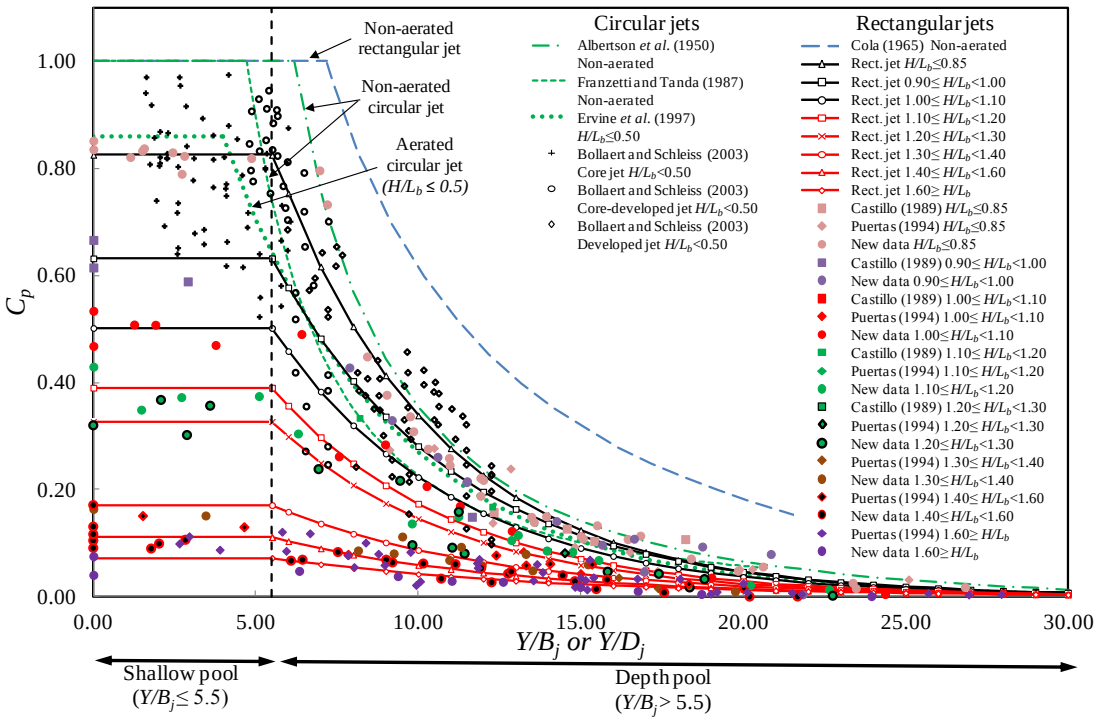

Figure 3: Mean dynamic pressure coefficient for different jet shapes and air entrainment

Figure 3 also shows the fit of the aerated circular jets obtained by Ervine *et al.* [22] and Bollaert and Schleiss [7], and non-aerated circular jets obtained by Albertson *et al.* [1] and those by Franzetti and Tanda [24]. In the same way as the Cola formula, the Albertson curve has been modified to consider the relation $C_p = f(Y/D_j)$ without the water cushion, being D_j the impingement diameter jet. For $Y/B_j > 5.5$, it was obtained that $C_p = f(Y/B_j, H/L_b)$. The C_p reduction is similar to a comparable circular jet.

For the effective water cushion ($Y > 5.5B_j$), eight cases have been considered as a function of the H/L_b ratio:

$$C_p = \frac{H_m - Y}{V_j^2/2g} = ae^{-b(Y/B_j)} \tag{11}$$

where H_m is the head mean registered at plunge pool bottom (stagnation point), Y the depth of the plunge pool and V_j the impingement velocity. The parameters a and b of the Eq. 11, and their regression adjustments R^2, are obtained from Table 1.

Table 1: Parameters of the mean dynamic pressure coefficient for $Y > 5.5B_j$

H/L_b	a	b	R^2
≤ 0.85	2.5	0.2	0.93
0.90-1.00	1.7	0.18	0.7
1.00-1.10	1.35	0.18	0.85
1.10-1.20	1.05	0.18	0.95
1.20-1.30	0.88	0.18	0.85
1.30-1.40	0.39	0.15	0.76
1.40-1.60	0.24	0.14	0.68
≥1.60	0.14	0.12	0.56

A study with the CFD code was also carried out. Three different specific flows (0.023, 0.037 and 0.058 m^2/s) and four water cushions (one non-effective and three effective water cushion depths) were analyzed. Results were compared with laboratory measurements and Parametric Methodology. Great similitude was obtained in the velocity of the free falling jet and the jet thickness. The distance from the weir to the stagnation point differed less than 2 % from the observed in laboratory and calculated with the Scimeni [44] formula.

Table 2 collects the pressure results obtained at the stagnation point with the weir crest located 2.35 m above the bottom of the plunge pool. In general, good agreement was obtained for the mean pressure coefficieants and the head mean with the three methodologies. Maximum differences among laboratory, Parametric Methodology and numerical results corresponded with direct impacts. In these cases, the pass from kinetic energy to potential energy is very abrupt, with significant pressure gradients appearing in reduced areas.

Considering the height between upstream water level and downstream water level, H, of each test, differences between simulations and laboratory data show a maximum error from -4% to 7%.

In these cases of direct impact, laboratory results revealed that the C_p is very sensitive to the H/L_b rate when H/L_b is between 0.70 and 1.30.

Table 2: Results obtained at the stagnation point

			CFD		LAB		PARAM.	
q (m^2/s)	Y (m)	H(m)	H_m (m)	C_p (-)	H_m (m)	C_p (-)	H_m (m)	C_p(-)
0.023	0.02	2.377	0.36	0.14	0.41	0.16	0.45	0.18
0.023	0.11	2.277	0.35	0.10	0.34	0.10	0.35	0.11
0.023	0.22	2.177	0.22	0.00	0.29	0.03	0.29	0.03
0.023	0.3	2.097	0.30	0.00	0.31	0.00	0.32	0.01
0.037	0.02	2.397	1.06	0.45	0.97	0.39	0.70	0.28
0.037	0.12	2.297	0.71	0.26	0.81	0.30	0.79	0.29
0.037	0.24	2.177	0.44	0.09	0.43	0.08	0.44	0.09
0.037	0.33	2.087	0.32	0.00	0.39	0.03	0.41	0.04
0.058	0.03	2.411	1.23	0.46	1.26	0.51	1.24	0.50
0.058	0.17	2.276	1.07	0.40	1.15	0.43	1.17	0.44
0.058	0.25	2.191	0.88	0.29	0.73	0.22	0.78	0.24
0.058	0.35	2.091	0.56	0.10	0.55	0.10	0.57	0.11

5.2 Velocity profiles in the plunge pool

To obtain the non-dimensional mean velocity profile in the hydraulic jump case (free and submerged), diverse authors (e.g. Görtler [25], Rajaratnam [42], [43], Hager [26], Ohtsu *et al.* [39], Wu and Rajaratnam [51], Liu *et al.* [32]) have obtained adjustment equations.

Supposing that V_j is the impingement velocity of the jet, B_j the jet thickness, and β the angle of the jet with the horizontal plane, Rajaratnam [43] carried out the dimensional analysis of the Reynolds-averaged Navier–Stokes equations and obtained the basic characteristics of the flow in a stilling basin.

Figures 4 and 5 show the horizontal mean velocity obtained in both, laboratory and numerical simulations, for a weir crest height of 2.35 m, diverse specific flows and water cushion depths together with the formulae proposed by some authors. Data have been divided by considering if the profile shows negative recirculation flow or if the entire velocity profile has direction to downstream.

The threshold between both behavior seems to be around 0.20-0.30 m of the stagnation point for the range of specific flows and water cushion depth analyzed. Data collapse for ratios $V_x/V_{max} \geq 0.40$. Under these value, results do not follow a single law. This is due to the jet enters into the plunge pool with an angle almost vertical, while the jet enters horizontally in the submerged hydraulic jumps downstream gates or spillways. The maximum differences among both behavior appear for the bigger water cushion (ratios $Y/B_j > 20$).

With these data, an adjustment has been proposed to define the non-dimensional velocity profile and the recirculation region of the inverse flow:

$$\frac{V}{V_{máx}} = 1.48\left(\frac{y}{\delta_l}\right)^{1/7}\left(1 - erf\left(0.66\frac{y}{\delta_l}\right)\right) \tag{12}$$

where *erf* is the error function, δ_l the characteristic length of the velocity distribution in the hydraulic jump (depth where $V_x = V_{max}/2$).

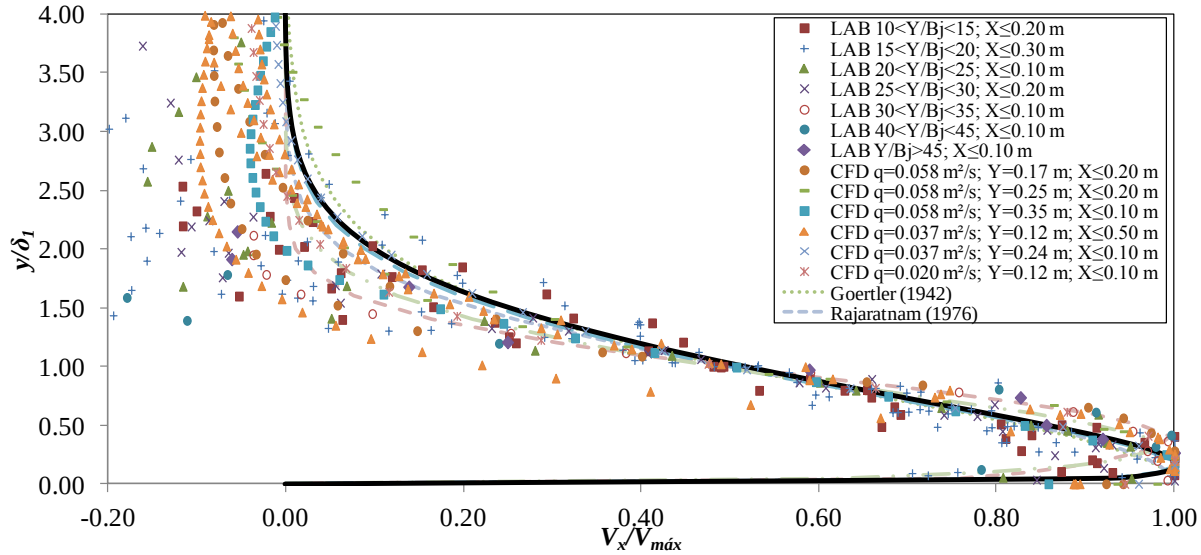

Figure 4: Distribution of the mean velocity downstream the stagnation point with laboratory data and numerical simulations. Profiles with negative flow

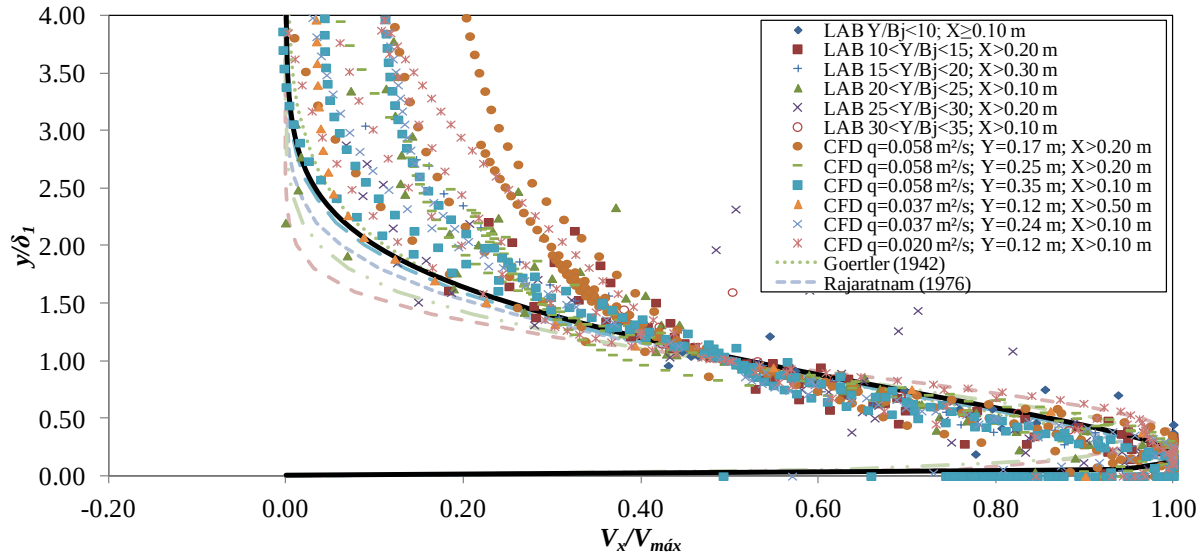

Figure 5: Distribution of the mean velocity downstream the stagnation point with laboratory data and numerical simulations. Profiles with positive flow

12 CONCLUSIONS

In the circular jet case, a transition region is considered between shallow and deep pool for ratios $4 < Y/B_j < 6$. In the nappe flow case, an effective water cushion is obtained when $Y/B_j > 5.5$. The maximum mean dynamic pressure coefficient is $C_p = 0.86$ in the case of circular jets,

while it is reduced to C_p = 0.83 for the rectangular jet case. With effective water cushions, tendencies are similar for both types of jets.

In the rectangular jet case, eight groups of C_p were obtained as a function of the H/L_b ratio, with ratios $0.8 \leq H/L_b \leq 1.60$. The results obtained complement the data of well-documented circular jets obtained from diverse authors.

In general, the results obtained with ANSYS CFX offered good agreement with the laboratory measurements and the Parametric Methodology. However, given that RANS turbulence models were used, the program obtained an average pressure register in contrast to the natural variability of the phenomenon which limited the possible analysis of fluctuant dynamic pressures.

Good agreement was obtained for the mean pressure coefficients and the head mean with laboratory results and Parametric Methodology. Considering the height between the upstream water level and downstream water level of each test, differences between simulations and laboratory data showed a maximum error from -4% to 7%.

The numerical results of the velocity profiles in the plunge pool downstream the stagnation point follow the laboratory data with differences smaller than 10% of the impingement velocity of the jet. However, these differences are significant in the aerated region. It was possible to adjust a velocity distribution for ratios $V_x/V_{max} \geq 0.40$. For smaller ratios it is necessary to consider different families of adjustments.

With the aim of improving the design of overtopping flows and their energy dissipation, it would be necessary to provide advances in the knowledge and characteristics of the hydrodynamic actions. More experimental studies, both in physical models and prototypes, are necessary in characterizing simultaneously the phenomena produced in the jets (aeration and velocity), combined with measurements of pressures, velocities and aeration rates in stilling basins.

In order to develop this work further, the researchers plan to examine use of inhomogeneous models and hence identify results independent from the mesh size. In future activities, comparison with diverse CFD codes (open source and commercial ones) will be considered.

ACKNOWLEDGEMENTS

The researchers express their gratitude for the financial aid received from the Ministerio de Economía y Competitividad and the Fondo Europeo de Desarrollo Regional (FEDER) through the Natural Aeration of Dam Overtopping Free Jet Flows and its Diffusion on Dissipation Energy Basins project (BIA2011-28756-C03-02).

REFERENCES

[1] M.L. Albertson, Y.B. Dai, R.A. Jenson and H. Rouse, Diffusion of submerged jets. *Proc. Int. Conf. ASCE,* **74**, (1950).
[2] G.W. Annandale, Erodibility. *J. Hydraulic Res.* **33**(4), 471-494, (1995).
[3] G.W. Annandale, *Scour Technology*. McGraw-Hill Professional, NY, USA, (2006).
[4] P. Asadollahi, F. Tonon, M.P.E.A. Federspiel and A.J. Schleiss, Prediction of rock block stability and scour depth in plunge pools. *J. Hydraulic Res.* **49**(6), 750-756, (2011).

[5] E.F.R. Bollaert, *Communication 13. Transient water pressures in joints and formation of rock scour due to high-velocity jet impact.* Laboratoire de Constructions Hydrauliques. Ed.: A.J. Schleiss, Ecole Polytechnique Fédérale de Lausanne, (2002).
[6] E.F.R., Bollaert and A.J. Schleiss, Scour of rock due to the impact of plunging high velocity jets Part I: A state-of the-art review. *J. Hydraulic Res.* **41**(5), 451-464, (2003).
[7] E.F.R., Bollaert and A.J. Schleiss, Scour of rock due to the impact of plunging high velocity jets Part II: Experimental results of dynamic pressures at pool bottoms and in one- and two-dimensional closed end rock joints. *J. Hydraulic Res*. **41**(5), 465-480, (2003).
[8] J.M. Carrillo, *Metodología numérica y experimental para el diseño de los cuencos de disipación en el sobrevertido de presas de fábrica*. PhD Thesis. Departamento de Ingeniería Civil, Universidad Politécnica de Cartagena, Spain, (2014). [in Spanish].
[9] L. Castillo, *Metodología experimental y numérica para la caracterización del campo de presiones en los disipadores de energía hidráulica. Aplicación al vertido libre en presas bóveda.* PhD Thesis. Departamento de Ingeniería Hidráulica, Marítima y Ambiental, Universidad Politécnica de Cataluña, (1989). [in Spanish].
[10] L. Castillo, Aerated jets and pressure fluctuation in plunge pools. *Proc. Int. Conf. The 7th International Conference on Hydroscience and Engineering (ICHE-2006),* Philadelphia, 1-23, M. Piasecki and College of Engineering, Drexel University, USA, (2006).
[11] L. Castillo, Pressure characterization of undeveloped and developed jets in shallow and deep pool. *Proc. 32nd IAHR Congress*, Venice, 2, 645-655, (2007).
[12] L. Castillo, J. Puertas and J. Dolz, Discussion of "Pressure fluctuations on plunge pool floors" by D.A. Ervine, H.T. Falvey and W.A. Withers. *J. Hydraulic Res.* **37**(2), 272-288, (1999).
[13] L. Castillo, J. Puertas and J. Dolz, Discussion of "Scour of Rock due to the impact of plunging high velocity jets. Part I: A state-of-the-art review" by E.F.R. Bollaert and A.J. Schleiss. *J. Hydraulic Res.* **45**(6), 853-858, (2007).
[14] L. Castillo and J.M. Carrillo, Numerical simulation and validation of hydrodynamics actions in energy dissipation devices. *Proc. 34th IAHR World Congress*, Brisbane, Australia, 1, 4416-4423, (2011).
[15] L. Castillo and J.M. Carrillo, Hydrodynamics characterization in plunge pools. Simulation with CFD methodology and validation with experimental measurements. *Proc. 2nd European IAHR Congress*, Munich, 1, (2012).
[16] L. Castillo and J.M. Carrillo, Analysis of the scale ratio in nappe flow case by means of CFD numerical simulation. *Proc. 35th IAHR World Congress*, Chengdu, China, 1, (2013).
[17] L. Castillo and J.M. Carrillo, Análisis numérico y experimental de velocidades en cuencos de aliviaderos de vertido libre. *Proc. 25 Congreso Latinoamericano de Hidráulica*, IAHR, Santiago, Chile, (2014). [in Spanish].
[18] L. Castillo, J.M. Carrillo and A. Blázquez, Plunge pool dynamic pressures: a temporal analysis in the nappe flow case. *J. Hydraulic Res* (in press), (2014).
[19] L. Castillo, J.M. Carrillo and A. Sordo-Ward, Simulation of overflow nappe impingement jets. *J. Hydroinformatics*, **16**(4), 922-940, (2014).
[20] R. Cola, Energy dissipation of a high-velocity vertical jet entering a basin. Proc. Int. *Conf. 11th International Association for Hydraulic Research Congress*, Leningrado, Ex-

USSR, 1, (1965).
[21] D.A. Ervine and H.R. Falvey, Behaviour of turbulent water jets in the atmosphere and plunge pools. *Proc. Int. Conf. Institutions of Civil Engineers*, **83**(2), 295-314, (1987).
[22] D.A. Ervine, H.T. Falvey and W.A. Withers, Pressure fluctuations on plunge pool floors. *J. Hydraulic Res.* **35**(2), 257-279, (1997).
[23] M.P.E.A. Federspiel, *Response of an Embedded Block Impacted by High-Velocity Jets*. PhD Thesis. Faculté environnement naturel, architectural et construit, École Politechnique Fédérale de Lausanne, Suisse, (2011).
[24] S. Franzetti and M.G. Tanda, Analysis of turbulent pressure fluctuation caused by a circular impinging jet. *Proc. Int. Conf. on New Technology in Model Testing in Hydraulic Research*, India, 85-91, (1987).
[25] H. Görtler. Berechnung von Aufgaben der freien Turbulenz auf Grund eines neuen Näherungsansatzes. *Journal of Applied Mathematics and Mechanics / Zeitschrift für Angewandte Mathematik und Mechanik - ZAMM*, **22**(5), 244–254, (1942). [in German].
[26] W. H. Hager, *Energy dissipators and hydraulic jump*. Vol. 8. Dordrecht, The Netherlands: Kluwer Academic Publ. Water Science and Technology Library, (1992).
[27] F. Hartung and E. Häusler, Scours, stilling basins and downstream protection under free overfall jets at dams. *Proc. Int. Conf. 11th Congress on Large Dams*, Madrid, Spain, 39-56, (1973).
[28] G.J.C.M. Hoffmans, Closure problem to jet scour. *J. Hydraulic Res.* **47**(1), 100-109, (2009).
[29] P. Horeni, *Disintegration of a free jet of water in air*. Byzkumny ustav vodohospodarsky prace a studie. Sesit 93, Praha, Pokbaba, (1956). [in Czech].
[30] B.E. Launder and B.I. Sharma, Application of the energy dissipation model of turbulence to the calculation of flow near a spinning disc. *Lett. Heat Mass Transfer* **1**(2), 131-138, (1972).
[31] A. Lencastre, *Descarregadores de lãmina livre: Bases para o seu estudo e dimensionamento*. Memoria Nº 174. Laboratorio Nacional de Engenharia Civil, Lisbon, (1961). [in Portuguese].
[32] P. Liu, J. Gao and Y. Li, Experimental investigation of submerged impinging jets in a plunge pool downstream of large dams. *Science in China*, **41**(4), 357-365, (1998).
[33] P.A. Manso, E.F.R. Bollaert and A.J. Schleiss, Dynamic pressures generated by plunging jets in confined pools under extreme flood discharges. *Proc. XXXI IAHR Congress*, Seoul, **1**, 2848-2860, (2005).
[34] P.A. Manso, E.F.R. Bollaert and A.J. Schleiss, Evaluation of high-velocity plunging jet-issuing characteristics as a basis for plunge pool analysis. *J. Hydraulic Res.* **46**(2), 147-157, (2008).
[35] F.R. Menter, Two-equation eddy-viscosity turbulence models for engineering applications. *AIAA J.* **32**(8), 1598-1605, (1994).
[36] M. Mehraein, M. Ghodsian and A.J. Schleiss, Scour formation due to simultaneous circular impinging jet and wall jet. *J. Hydraulic Res.* **50**(4), 395-399, (2012).
[37] J.F. Melo, A.N. Pinheiro and C.M. Ramos, Forces on Plunge Pool Slabs: Influence of Joints Location and Width. *J. Hydraulic Eng.* **132**(1), 49-60, (2005).
[38] W.L. Moore, Energy loss at the base of a free overall. *Transactions, American Society of Civil Engineering*, **108**(1), 1343-1360, (1943).

[39] F. Ohtsu, Y. Yasuda and S. Awazu, *Free and submerged hydraulic jumps in rectangular channels.* Report of the Research Institute of Science and Technology. Nihon University. No 35, (1990).
[40] J. Puertas, *Criterios hidráulicos para el diseño de cuencos de disipación de energía en presas bóveda con vertido libre por coronación*. PhD Thesis. Departamento de Ingeniería Hidráulica, Marítima y Ambiental, Universidad Politécnica de Cataluña, Spain, (1994). [in Spanish].
[41] J. Puertas and J. Dolz, Plunge pool pressures due to falling rectangular jet. *J. Hydraulic Eng.* **131**(5), 404–407, (2005).
[42] N. Rajaratnam, The hydraulic jump as wall jet. *Proc. ASCE, Journal of Hydraulic Division. 91(HY5)*, 107-132, (1965).
[43] N. Rajaratnam, *Turbulent jets*. Elsevier Scientific, Development in Water Science, 5 New York, USA, (1976).
[44] E. Scimeni, Sulla forma delle vene tracimanti. *L´Energia Elettrica*, **7**(4), 293-305, (1930). (in Italian).
[45] B. Stutz and J.L. Reboud, Experiment on unsteady cavitation. *Exp. Fluids* **22**, 191-198, (1997).
[46] B. Stutz and J.L. Reboud, Two-phase flow structure of sheet cavitation. *Phys. Fluids* **9**(12), 3678-3686, (1997).
[47] T.L. Wahl, K.H. Frisell and E.A. Cohen, Computing the trajectory of free jets. *J. Hydraul. Eng.* **134**(2), 256-260, (2008).
[48] L. Wasewar and J. Vijay Sarathi, CFD modelling and simulation of jet mixed tanks. *Eng. Appl. Comp. Fluid Mech.* **2**(2), 155-171, (2008).
[49] D.C. Wilcox, *Turbulence modeling for CFD*, 3rd edition. DCW Industries, Inc., La Canada, California, (2006).
[50] W. Withers, *Pressure fluctuation in plunge pool of an impinging jet spillway*. PhD Thesis. Department of Civil Engineering, University of Glasgow, United Kingdom, (1991).
[51] S. Wu and N. Rajaratnam, Free jumps, submerged jumps and wall jets, *J. of Hydraulic Research*, **33**(2), 197-212, (1995).